Proceedings of ASME Turbo Expo 2011
GT2011
June 6-10, 2011, Vancouver, British Columbia, Canada

GT2011-46177

AN INVESTIGATION OF THE FLOW STRUCTURES AND FLOW CONTROL IN A VARIABLE GEOMETRY TURBINE

Lei Huang, Weilin Zhuge, Yangjun Zhang
State Key Laboratory of Automotive Safety and Energy
Tsinghua University
Beijing 100084, China

Lifeng Hu
National Key Laboratory of
Diesel Engine Turbocharging Technology
Datong, Shanxi 037036, China

ABSTRACT

The flow structures of a variable geometry turbine at operating conditions of different nozzle open positions were investigated through CFD simulations. The flow field structures of the VGT at highly off-design operating conditions were presented. The evolution of the secondary flow vortex structures was studied.

CFD results show that at open nozzle position, there is a recirculation zone on the nozzle vane pressure surface, and the rotor blade is under a considerable negative incidence, which leads to a passage vortex on the pressure surface of the blade. At closed nozzle position, the flow into the rotor has positive incidence, which leads to a recirculation zone on the suction surface. At highly off-design conditions, the passage vortex caused by the misalignment of the rotor inlet flow angle and the rotor blade angle accounts the most important losses of turbine flow.

The turbine flow was controlled by adjusting the blade inlet angle distribution along the leading edge while keeping the radial-fiber rotor construction. CFD simulations show that the turbine efficiencies are improved in most operating points at both open and closed nozzle conditions.

NOMENCLATURE

CFD	Computational Fluid Dynamics
VGT	Variable Geometry Turbine
VNT	Variable Nozzle Turbine
MFR	Mass Flow Rate
EGR	Exhaust Gas Recirculation
NOx	Nitrogen Oxides
PM	Particulate Matter

1 INTRODUCTION

Turbocharging is one of the most important technologies for automotive engine performance improvement. VGT plays a key role in the emission control systems such as EGR to control the engine NOx and PM emissions [1]. VGT can adapt to the exhaust gas flow conditions under different engine operating conditions, by varying the nozzle opening. Since VGT is mostly operated under highly off-design conditions on the engine, it is important to study the aerodynamics and performance of VGT at off-design conditions.

Hideaki Tamaki et al [2] found the leakage flow in the tip clearance of the nozzle vane of VGT significantly affected the flow field downstream of the nozzle vane at the smallest nozzle opening condition. At largest nozzle opening condition, the effect of leakage flow is small and the effect of wake is dominant. The leakage vortex leads to non-uniformity distribution of the total pressure and flow angle in the entire pitch direction, which causes the mixing loss downstream of the nozzle vane and deteriorates the turbine performance.

Jason Walkingshaw et al [3] carried out a numerical study on a scaled automotive VGT at highly off-design conditions. The flow fields were investigated at the maximum, minimum and 25% MFR conditions. The CFD analysis revealed that at maximum MFR (the design point) the approaching flow is well aligned with the stator vanes and the rotor and the tip leakage causes the flow separation in the rotor passage. At minimum MFR, due to the poor inlet flow alignment, a strong separation presents on the rotor blade suction surface and causes a poor flow in the rotor passage.

Segawa et al [4] investigated the balance of nozzle flow capacity and rotor flow capacity of VGT by CFD analysis. They found the ratio of nozzle throat area to rotor throat area greatly influences turbine efficiency and maximum flow capacity. A VGT with best balance of nozzle and rotor capacity was designed and showed wide flow range and high efficiency.

In order to improve the efficiency of radial turbine at off-design condition, the backswept blading turbine design was investigated by Liam Barr et al [5, 6]. The CFD results showed that with the backswept blade the flow separation on the suction was reduced since the backswept blade is able to cope with the strong positive incidence at rotor inlet at off-design condition. The efficiency of the turbine with 25° backswept blade is 1.76% higher than the baseline radial turbine at approximately 50% of the design speed.

Backswept blading can improve the VGT efficiency at off-design conditions. However, since backswept blading results in a non-radial-fiber impeller, the blade stress level increases with the backswept angle, and the efficiency improvement would be limited by the blade stress lever.

In this paper, the internal flow fields of vane and blade passages at highly off-design points were analyzed by CFD simulations. The evolution of the secondary flow vortex structures and the flow losses distribution in the rotor passage were analyzed. The turbine blade design was improved through modification of the blade inlet angle distribution along the leading edge while keeping the radial-fiber rotor construction. The performance of the modified turbine was compared to the original turbine at different nozzle open positions by CFD analysis.

2 NUMERICAL MODEL

The geometry of the variable geometry turbine is shown in Figure 1. The VGT has 11 nozzle vanes and 9 impeller blades. Each vane can be rotated about its pivot axis.

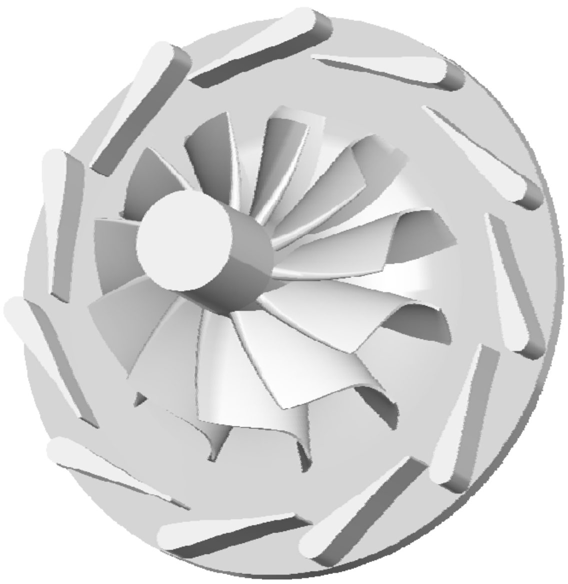

Figure 1. Geometry of the variable geometry turbine

The CFD simulations were performed using the commercial NUMECA code. The nozzle and the rotor are simulated together. A 3-passage simulation and a single passage simulation were conducted. There is no significant difference between the 3-passage and single passage simulation results. Hence the single passage simulations were conducted for further investigations. The computation grid cell numbers of the stator and rotor meshes are more than 320000 and 619000 respectively, with almost 940000 cells in total, which was more than the minimum requirement indicated by the grid independence study. In order to effectively capture the complex 3D flow patterns within the flow passage, an HO-topology and HC-topology were used in stator and rotor passage respectively. H-topology was used in the inlet, outlet and main flow passage domains. The grid topologies of skin blocks around the stator vane and rotor blade are O-topology and C-topology respectively. The grid was refined at the near-wall, leading and tailing edge regions. The minimum skew angle of grid cells was 25.7^{o}. The rotor blade tip clearance is 0.4 mm. The clearance region is meshed by 13 grid points in span wise direction. The computational grids are shown in Figure 2.

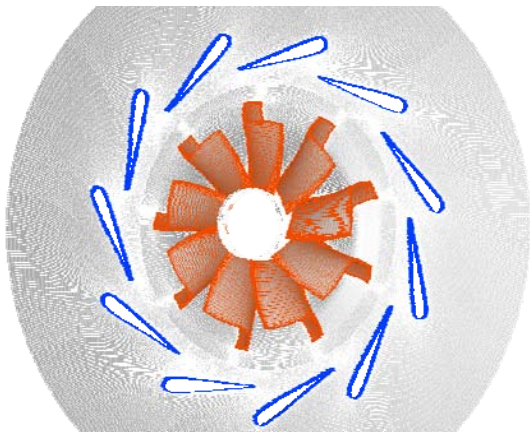

Figure 2. Computational grids of the turbine

At inlet boundary, the velocity direction, static temperature and mass flow were specified. At outlet boundary, the static pressure was specified. The flow angle was fixed at the inlet boundary, which value was calculated according to the volute geometry. The mixing plane interface was used at the nozzle-rotor stage interface, which guarantees an exact conservation of mass flow, momentum and energy through the interface. Sparlart-Allmaras model was used for the turbulence mode. The y+ value of the wall-adjacent cells was controlled less than 10 in order to capture the highly gradient flow within the boundary layer.

3 PERFORMANCE SIMULATION RESULTS

CFD simulations were carried out at the rotating speeds of 150000 rpm for three different nozzle open positions: "closed", "medium" and "open" positions. Figure 3 shows the CFD performance predictions of mass flow rate and efficiency against pressure ratio at three different nozzle open positions. It is shown that at "open" nozzle position the highest efficiency is much lower than that at "medium" and "closed" nozzle positions.

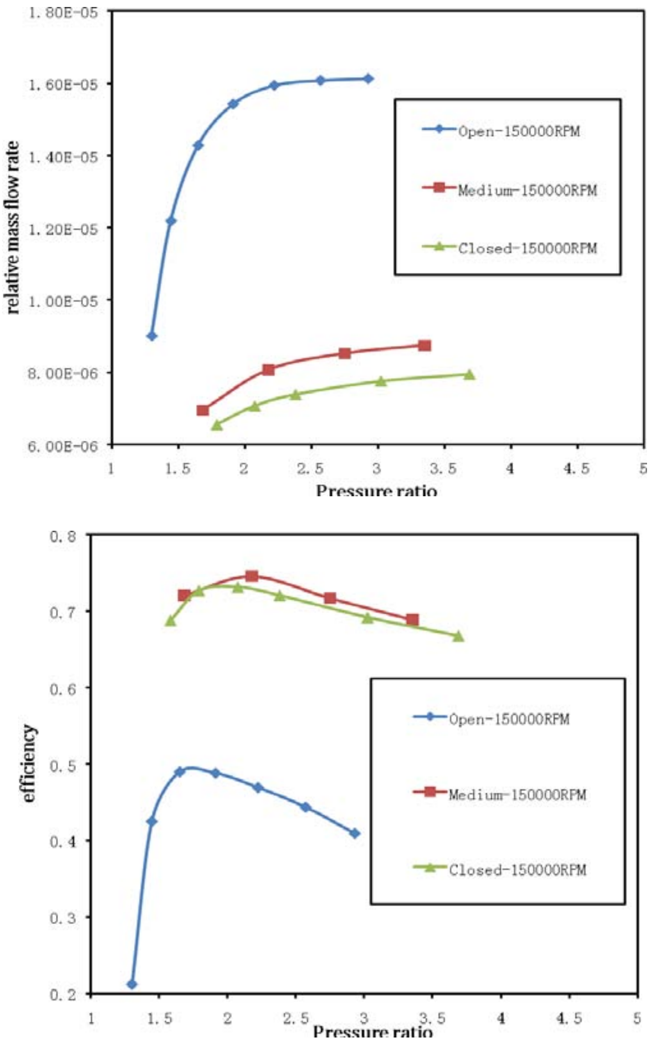

Figure 3. Stage performance characteristics predicted by CFD simulations

4 THE INTERNAL FLOW FIELDS AT DIFFERENT NOZZLE POSITIONS

The influence of different nozzle open positions on the steady flow field was analyzed at the same pressure ratio of 1.7, where the efficiencies of the turbine are relatively high.

4.1 THE INTERNAL FLOW FIELDS AT OPEN NOZZLE POSITION

Figure 4 shows the Mach number contour and streamline distribution of 50% spanwise plane at open nozzle position. A zone of recirculation generated on the pressure surface of the nozzle, as shown in Figure 4. The recirculation zone reduces the effective flow area of nozzle passage. The trailing edge wake of the nozzle is weak and the nozzle outlet flow is considerably uniform in the circumference direction. Although there is a recirculation zone in the nozzle passage, the flow losses in vane passage accounts only about 14.8% of the total losses. The main loss occurs in the rotor blade passage.

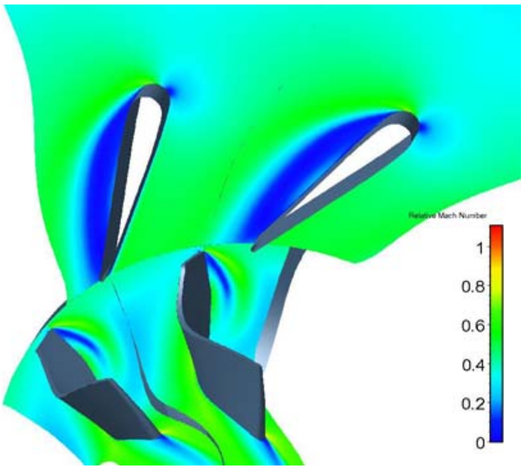

(a) Mach contour

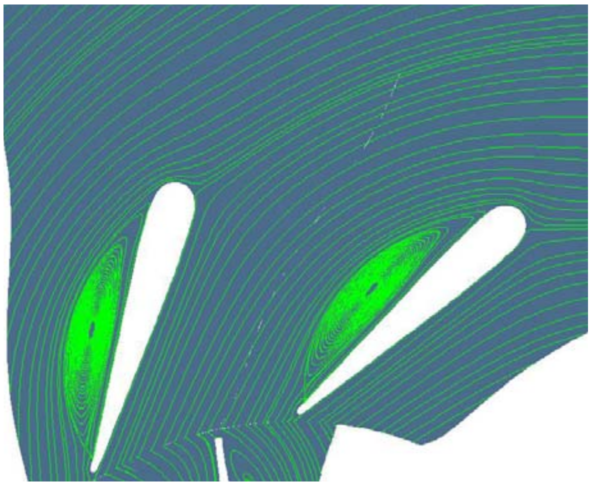

(b) Streamline distribution

Figure 4. Mach contour and streamline distribution at 50%span

Figure 5 shows streamline distributions of the primary flow characteristics on various span planes located between the hub and shroud of the rotor at nozzle open condition. The rotor blade is under a considerable negative incidence. At 5% span and 50% span planes, a recirculation zone generates on the pressure surface, which occupies a certain area of the blade inlet region. In the plane near the hub the recirculation zone is smaller in size. At 95% span plane, the blade tip clearance flow influences the flow separation on the blade pressure surface and moves from the pressure surface to the suction surface and a small quantity of flow passes through the tip gap corresponding to flow motion shown in Figure 5(d). At the suction surface near the hub, a vortex appears since the flow passing over the

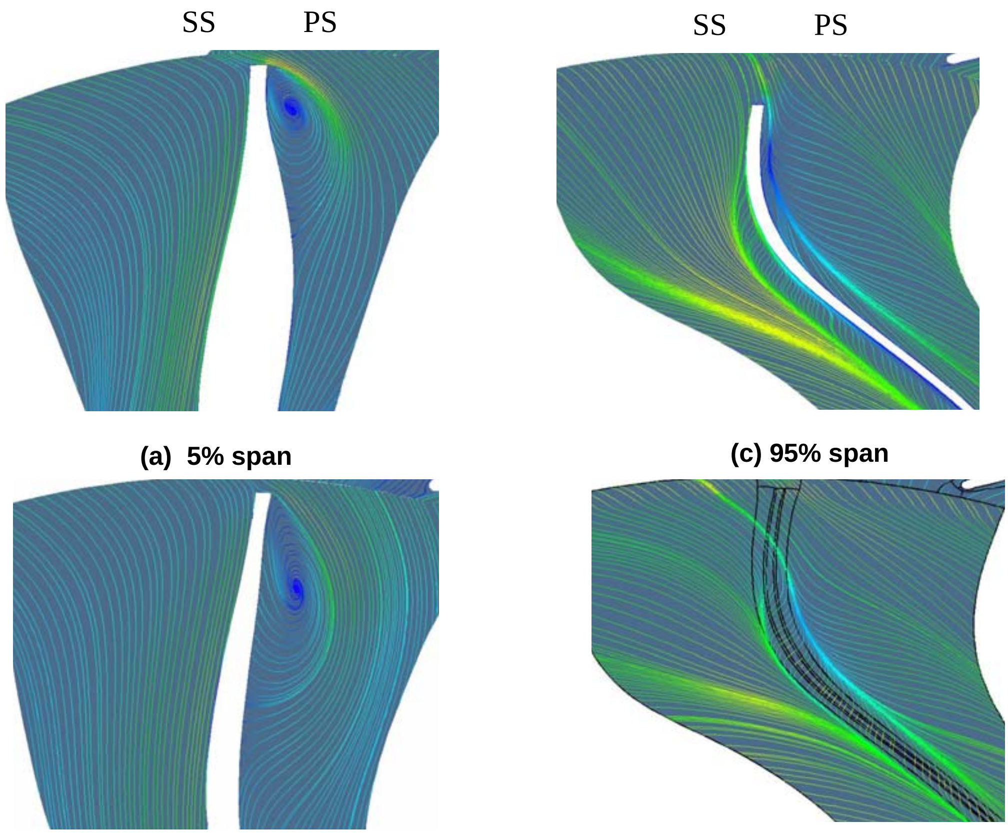

(a) 5% span

(c) 95% span

(b) 50% span

(d) 99.5% span

Figure 5. Streamline distribution plots on various span planes (open nozzle position)

no flow reversal exists. A flow attachment line starts from the leading edge to the trailing edge near the pressure surface, while a flow separation line starts at 20% chord approximately proceeding to the exducer on the suction surface. The streamline distribution of 99.5% span plane shows that the fluid is driven from the suction surface to the pressure surface from the leading edge to 20% chord approximately because of the negative incidence at the rotor inlet, and the fluid is driven from the pressure surface to the suction surface through the clearance from the 20% chord approximately to the trailing edge because of the positive pressure gradient.

Figure 6 shows the streamline distributions of the secondary flow and the contours of the entropy generation on different streamwise planes. The blade rotates in the anticlockwise direction. The pressure surface of the blade is on the right and the suction surface is on the left, and the shroud is at the top and the hub is at the bottom in the figures.

At the plane near the inlet, due to the negative incidence at the rotor inlet and the relative motion of the shroud, the fluid leading edge mixes with the main flow. There is no obvious tip leakage vortex existing at this plane. The entropy generation contour shows that the main loss occurs on the pressure surface due to the flow separation.

At 25% chord, a big passage vortex rotating in the clockwise direction is developed and occupies the main passage close to the pressure surface. Another vortex is generated under the passage vortex and rotates in the opposite direction. The fluid is driven from the pressure surface to the suction surface through the tip clearance. At 75% chord, the passage vortexes disappear and the tip leakage vortex is formed in the blade tip on suction surface. The main entropy generation is caused by the tip leakage flow. At the streamwise plane adjacent to the outlet, the tip leakage vortex dominates the flow field.

4.2 THE INTERNAL FLOW FIELDS AT CLOSED NOZZLE POSITION

At closed nozzle position, the stage efficiency is much higher than the open nozzle position, as shown in Figure 3. The

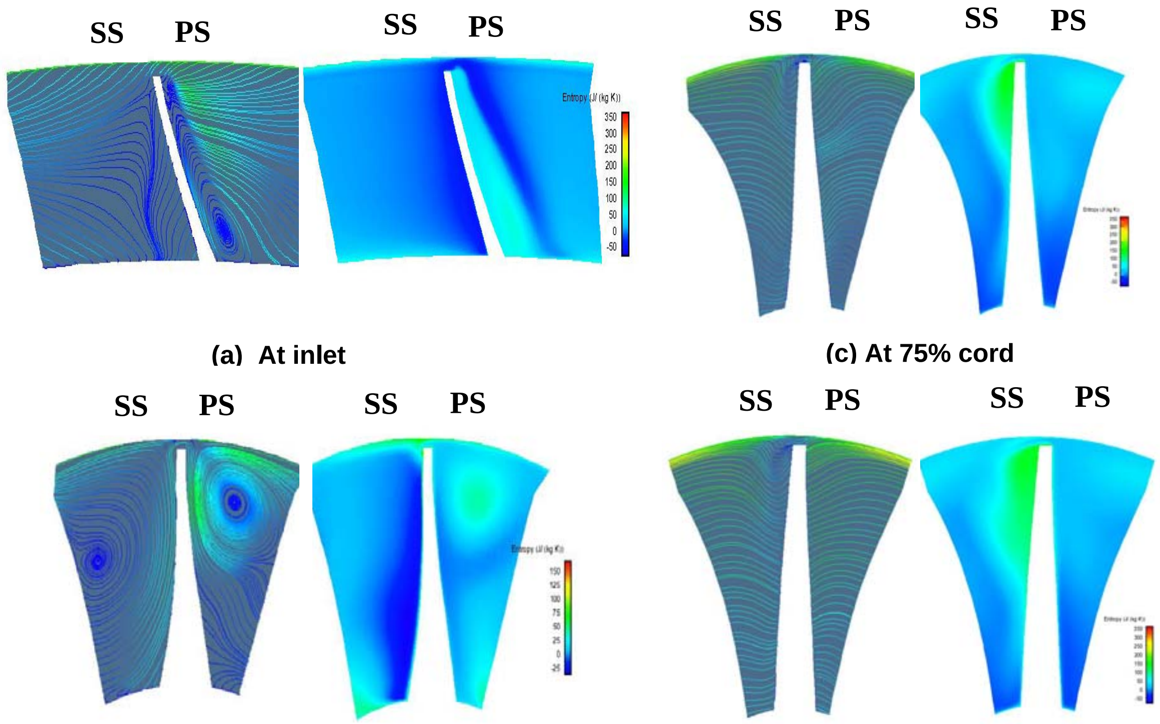

(a) At inlet **(c) At 75% cord**

(b) At 25% cord **(d) At outlet**

Figure 6. Streamline distributions and entropy generation contours (open nozzle position)

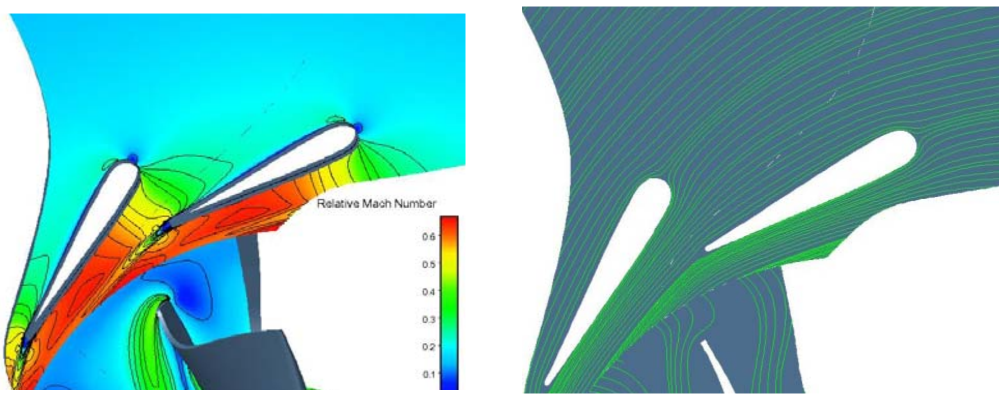

(a) Mach contour **(b) Streamline distribution**

Figure 7. Mach contour and streamline distribution at 50% span

flow at the inlet of the nozzle aligns well with the nozzle vanes. There is no recirculation zone in the nozzle passage, as shown in Figure 7. The velocity in the nozzle passage is higher, due to the narrow throat area, leading to the non-uniform flow at the outlet of the nozzle vanes. Figure 7 shows the strong trailing edge wake, which is the main cause of the flow non-uniformity outlet of the nozzle. Fortunately, increase of nozzle vane angle will increase the vaneless space between the nozzle and the rotor, which will decrease the circumferentially flow non-uniformity into the rotor [7]. The loss of nozzle passage accounts about 14.5% of the total stage loss, nearly the same as the open nozzle condition.

Figure 8 shows the flow structures at different spanwise planes at closed nozzle condition. The flow structures are totally different from the case of open nozzle condition. The flow into the rotor has positive incidence, which leads to a

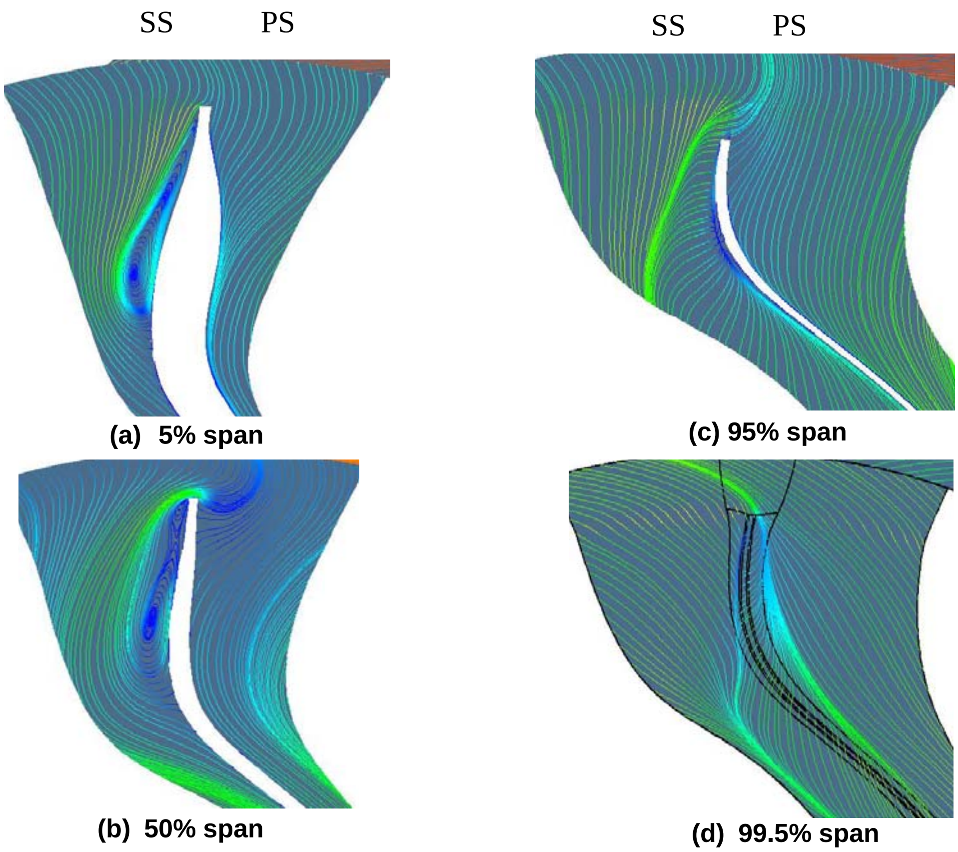

Figure 8. Streamline distribution plots on various span planes (closed nozzle position)

recirculation zone generated on the suction surface. The recirculation zone extends from the leading edge to the 35% chord approximately. At 5% span the recirculation zone is reduced in size and extends further downstream of the blade passage, as shown in Figure 8(a). At the span near the blade tip the vortex disappears and a flow separation line appears from the leading edge of the suction surface and proceeds to the blade passage, as shown in Figure 8(c). It is caused by the blade tip leakage flow from the pressure surface to the suction surface, as shown in Figure 8(d).

Figure 9 shows the streamlines distributions of the secondary flow and the contours of the entropy generation at different streamwise planes. At the plane near the inlet, flow almost moves from the suction surface to the pressure surface due to the positive incidence. Flow near the shroud is turned due to the relative motion of the shroud wall, which causes complex flow field on the suction surface. The flow on the pressure surface turns to move to the tip along the blade surface due to the pressure gradient on the pressure surface, as shown in Figure 9(a). According to the entropy generation contour in Figure 9(a), the main loss appears on the suction surface where a bubble separation occurs.

At 25% chord, a passage vortex appears on the suction surface rotating in the clockwise direction. Another vortex rotating in anticlockwise direction is generated near the shroud side on the suction surface caused by the tip leakage flow and the scraping effect of the shroud. Losses are mainly caused by the passage vortex and the strong tip leakage flow, as shown in the entropy generation contour in Figure 9(b).

At 75% chord, the passage vortexes disappear and the tip leakage vortex is formed in the blade tip on suction surface, which is larger than in the case of open nozzle condition, as shown in Figure 9(c).

At the outlet plane, the flow pattern is much simple and the secondary flow is mainly from the suction surface to the pressure surface. The flow field is dominated by the blade tip leakage vortex. The effect of the tip leakage vortex leads to the main losses indicated by the entropy generation contour in Figure 9(e).

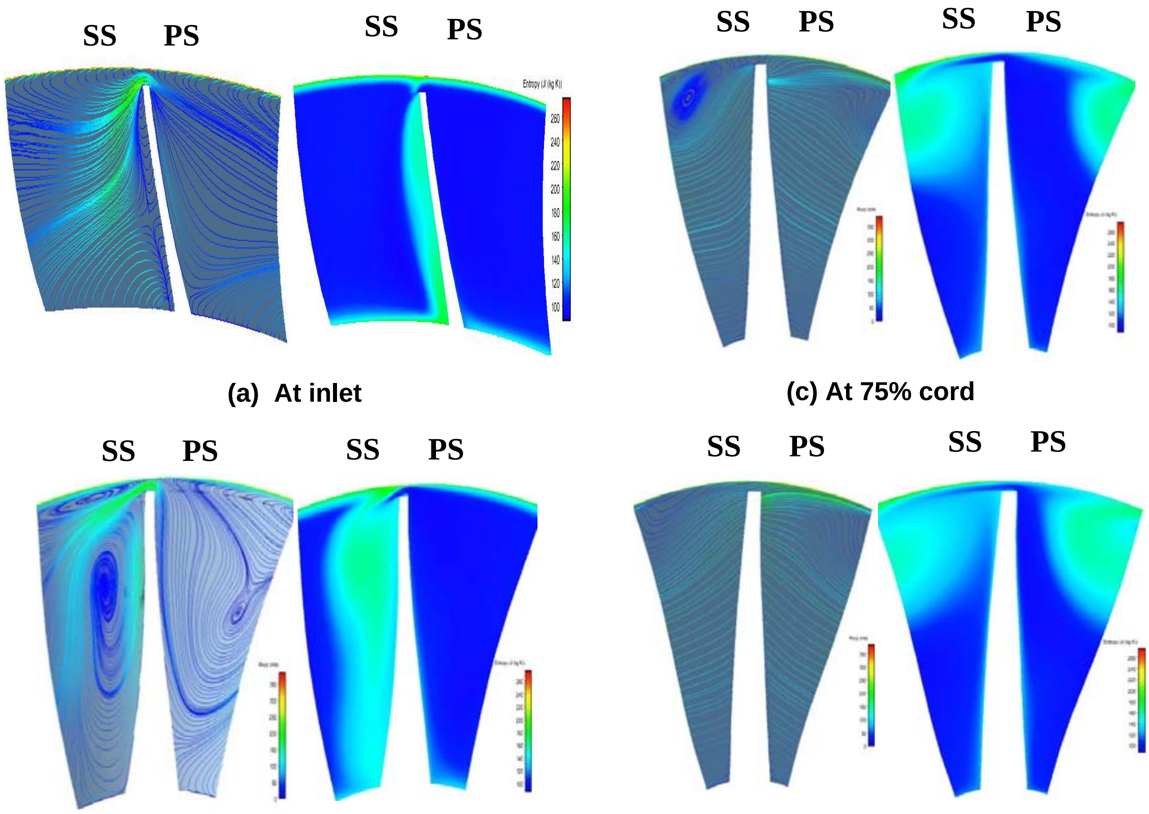

(a) At inlet

(c) At 75% cord

(b) At 25% cord

(d) At outlet

Figure 9. Streamline distributions and entropy generation contours (closed nozzle position)

5 FLOW CONTROL OF THE VARIABLE GEOMETRY TURBINE

According to the CFD analysis of the flow structures at open and closed nozzle positions, the passage vortex near the leading edge of the rotor blade is the main causes of the flow loss at off-design conditions. The passage vortex is caused by the misalignment of the rotor inlet flow angle and the rotor blade angle. However, simply modify the rotor blade inlet angle would result in a non-radial-fiber rotor and introduce additional bending stresses.

Adjusting the blade inlet angle distribution along the blade leading edge could modify the blade inlet angle while keeping the radial-fiber rotor construction. The original turbine blade inlet angle distribution was modified to control the flow separation at the leading edge and achieve better performance characteristic. The geometry of the modified rotor blade is shown in Figure 10.

Figure 11 shows the performance comparison of new turbine design and the original design at open and closed nozzle positions by CFD simulations. At operating condition of open nozzle position, the turbine efficiency is improved at full operating range, the largest efficiency improvement is up to 5% at pressure ratio of 1.7. At closed nozzle position, the turbine efficiency is also improved at the low pressure ratio conditions, which corresponds to the turbine normal operating conditions.

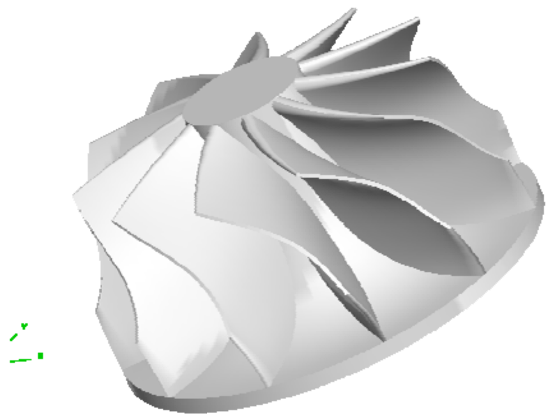

Figure 10. The geometry of the modified rotor blade

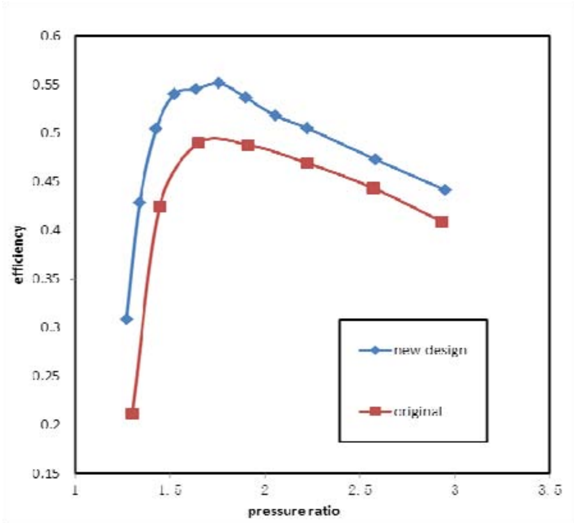

(a) open nozzle position

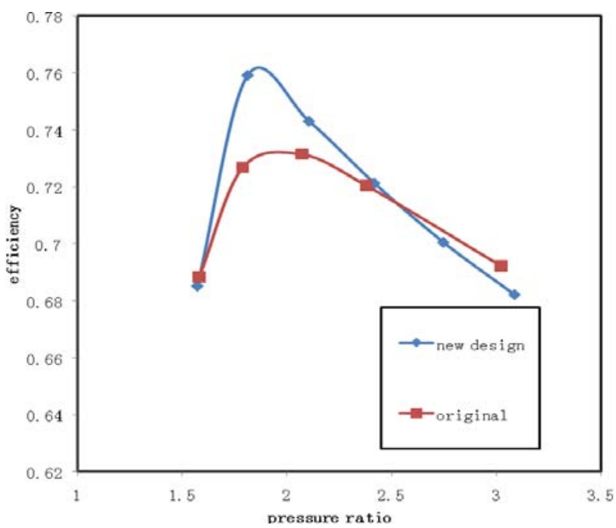

(b) closed nozzle positoin

Figure 11. Comparison of eefficiency characteristic of the new designed and original turbine

The flow structures of the new turbine and original turbine at the 50% span of the blade passage were compared in Figure 12. There is a recirculation zone generated on the pressure surface in both two turbines. The new turbine adapts to the negative flow incidence better, and recirculation zone is smaller. The blade passage flow field of the new turbine is much smoother than the original one.

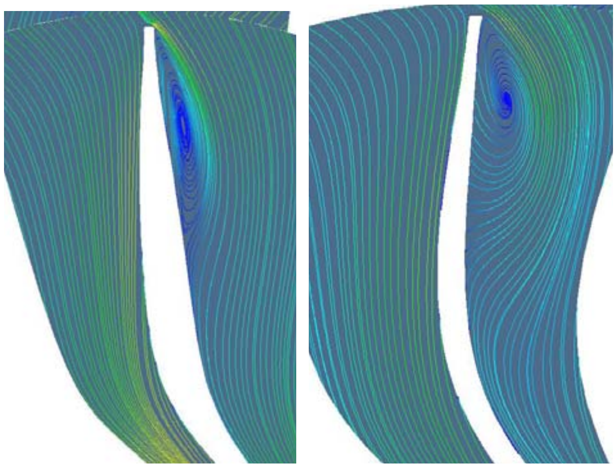

(a) the new design (b) the original

Figure 12. Streamlines distribution at 50%span

6 CONCLUSIONS

With the VGT used more and more in the automotive engines, it should be better to understand the performance characteristic of VGT in different operating conditions. Since the VGT frequently operates at off-design conditions, it is necessary to study the flow structures at those conditions. CFD simulations were carried out on a VGT at operating conditions of different nozzle open positions. The internal flow fields of vane and blade passages at open and closed nozzle vane position were analyzed.

At open nozzle position, there is a recirculation zone generated on the nozzle vane pressure surface. Though the trailing edge wake is weak and the flow into the rotor is relatively uniform, the nozzle outlet flow is not very well aligned with the rotor blade. At this condition the rotor blade is under a considerable negative incidence, which leads to a passage vortex existed on the pressure surface of the blade. The tip leakage vortex is formed at 50% chord with limited influence on the turbine performance. Main losses are caused by the passage vortex in one half of rotor passage and the tip leakage flow in another half of rotor passage.

At closed nozzle position, the inlet flow is better aligned with the nozzle vanes and there is no recirculation zone in the nozzle passage. The high flow velocity due to the narrow nozzle throat area in the nozzle passages leads to the non-uniform flow at the outlet of nozzle. The flow into the rotor has positive incidence, which leads to a recirculation zone generated on the suction surface. The tip leakage vortex is stronger due to the higher pressure gradient. Losses mainly occur on the suction surface caused by the passage vortex and the strong tip leakage flow.

A new turbine rotor was designed by modifying the blade inlet angle distribution along the leading edge while keeping the radial-fiber rotor construction. CFD simulations show that the turbine efficiencies are improved in both open nozzle conditions and closed nozzle conditions, despite of a little efficiency drop at high pressure ratio operating conditions at closed nozzle position.

ACKNOWLEDGMENTS

The authors would like to thank the National Basic Research Program of China (2011CB707204) for the support.

REFERENCES

[1] Tomoki Kawakubo, 2010, "Unsteady Rotor-Stator Interaction of a Radial-Inflow Turbine With Variable Nozzle Vanes". Proceedings of ASME Turbo Expo 2010: Power for Land, Sea and Air.

[2] Hideaki Tamaki, Shinya Goto, Masaru Unno, Akira Iwakami, 2008, "The Effect of Clearance Flow of Variable Area Nozzles on Radial Turbine Performance". Proceedings of ASME Turbo Expo 2008: Power for Land, Sea and Air.

[3] Jason Walkingshaw, Stephen Spence, Jan Ehrhard, David Thornhill, 2010, "A Numerical Study of the Flow Fields in a Highly Off-Design Variable Geometry Turbine". Proceedings of ASME Turbo Expo 2010: Power for Land, Sea and Air.

[4] K. Segawa, A. Iwakami, S. Yamaguchi, H. Tange, K. Kimachi, 2010, "Improvement of Turbine Performance for Small Size Variable Geometry System Turbocharger". 9th International Conference on Turbochargers and Turbocharging.

[5] Liam Barr, Stephen Spence, Paul Eynon, 2008, " Improved Performance of a Radial Turbine through the Implementation of Back Swept Blading". Proceedings of GT2008 ASME Turbo Expo 2008: Power for Land, Sea and Air.

[6] Liam Barr, Stephen Spence, David Thornhill, Paul Eynon, 2009, "A Numerical and Experimental Performance Comparison of an 86mm Radial and Back Swept Turbine". Proceedings of ASME Turbo Expo 2009: Power for Land, Sea and Air.

[7] Alister Simpson, Stephen Spence, John Watterson, 2008," Numerical and Experimental Study of the Performance Effects of Varying Vaneless Space and Vane Solidity in Radial Inflow Turbine Stators". Proceedings of ASME Turbo Expo 2008: Power for Land, Sea and Air.

